A NOTE ON A MICROPROCESSOR-BASED RECORDING CURRENT METER SUITABLE FOR WAVE RESEARCH

P.F. Hamblin, J.A. Bull and F. Chiocchio

NWRI Contribution No. 89-54

Lakes Research Branch
National Water Research Institute
Canada Centre for Inland Waters
Burlington, Ontario, Canada L7R 4A6

Environment Canada

ABSTRACT

The need to determine bed shear stresses as required for estimation of resuspension and deposition of fine-grained sediments and their associated contaminant transport has in shallow lakes and nearshore areas called for the measurement of wave data as well as mean flows according to recent theories of wave-current interaction. Wave statistics recorded over a two-week period in a wave dominated shallow lake at two depths by a vector-averaging current meter are compared to independently measured wave data. Wave orbital motions are within 3% of those determined by spectral analysis of frequently sampled currents. Wave propagation directions are within ±19 degrees of spectrally determined directions and qualitatively similar to the fetch weighted wind direction. Less satisfactory agreement was evident between the wave periods as determined by zero-crossings and the wave spectral peak periods. Reasonable wave periods could only be inferred when the RMS orbital speed exceeded the mean speed. Another possible algorithm for evaluating wave period is tested and recommendations are made for impovements of the measurement system.

RÉSUMÉ

La détermination des contraintes de cisaillement des couches requise pour évaluer la remise en suspension et le dépôt des sédiments à grains fins ainsi que le transport connexe des contaminants a nécessité, pour les lacs peu profonds et les zones côtières, la mesure des données sur les vagues ainsi que sur les débits moyens selon les récentes théories de l'interraction vague-courant. Les statistiques relatives aux vagues, enregistrées au cours d'une période de deux semaines, dans un lac peu profond dominé par les vagues, à deux profondeurs, à l'aide d'un courantomètre calculant la moyenne vectorielle sont comparées avec les données sur les vagues mesurées indépendemment. Les mouvements orbitaux s'écartent de 3 % de ceux déterminés par l'analyse spectrale des courants fréquemment échantillonnés. Les directions de propagation des vagues se situent à ± 19 degrés des directions déterminées spectralement et sont qualitativement semblables à la direction du vent pondérée en fonction du fetch. La concordance était moins satisfaisante entre les périodes des vagues mesurées par les passages à zéro et les périodes de pointe spectrale des vagues. Des périodes de vagues raisonnables n'ont pu être déduites que lorsque la vitesse orbitale RMS dépassait la vitesse moyenne. On fait actuellement l'essai d'un autre algorithme possible pour l'évaluation de la période des vagues et on formule des recommandations visant à apporter des améliorations au système de mesure.

MANAGEMENT PERSPECTIVE

The need for the measurement of the transport of suspended sediments in the nearshore areas of large lakes or in open waters of shallow lakes where wave forces are important has called for the development of new instrumentation. A version of the current meter (SACM) has been extended in our laboratory to record wave orbital motion, wave direction and period, along with the conventional current speed, direction and water temperature. Field deployment and critical evaluation have shown that while wave orbital motion and wave direction are adequately sampled there is need for improvement in wave period. Another method of wave period estimation is evaluated and recommendations are made for future development of the microprocessor-based current meter.

PERSPECTIVE - GESTION

La mesure du transport des sédiments en suspension dans les zones côtières des grands lacs ou dans les eaux libres des lacs peu profonds, soumis à de fortes vagues, a nécessité la mise au point de nouveaux instruments. Le courantomètre (SCAM) a été amélioré dans notre laboratoire pour enregistrer le mouvement orbital des vagues, leur direction et leur période, ainsi que la vitesse et la direction conventionnelles du courant et la température de l'eau. Le déploiement sur le terrain et l'évaluation critique ont indiqué que, bien que le mouvement orbital et la direction des vagues soient correctement échantillonnés, il faut encore améliorer l'évaluation de la période des vagues. On évalue actuellement une autre méthode d'évaluation de la période des vagues et on formule des recommandations pour la future mise au point du courantomètre relié à un microordinateur.

INTRODUCTION

The need to investigate the role played by suspended sediments in the transport and fate of contaminants in the lacustrine environment has led to the measurement of currents in shallow lakes and in the nearshore zone where surface wave influences are crucial to the dynamics of sediment resuspension. In these areas the peak bed shear stress is considered to be related to sediment resuspension. In turn, the bed shear stresses according to wave-current interaction theories of Christoffersen and Jonsson (1985) and Grant and Madsen (1979) are related to wave period, direction and orbital motion. With the development of rapid response current sensors it is possible to measure the wave orbital motions with periods as short as several seconds characteristic of lakes. For example, Hamblin et al. (1987) reported wave orbital motions with periods of three seconds in their 1985 field study of Lake St. Clair employing an electromagnetic current meter. Unfortunately, the currently available recording capability permitted the collection of only 160 bursts of rapidly sampled data. In a lake wave events may respond to atmospheric forcing over periods as short as one-half an hour so that such systems are unsuitable for long-term unattended deployments of typical durations of six weeks or more, as is the case with conventional current meters.

As another component of the above-mentioned field study, we successfully deployed a rapid response acoustic current meter of Neil Brown manufacture (Bull and Valdmanis, 1986). Instead of recording all the 0.5-s samples, mean components of currents over bursts from 5 to 10 minutes in length are computed by a microprocessor on board the current meter thus saving on recording capacity and greatly extending the duty cycle of the instrument. Our estimates showed that there is sufficient storage in the memory of the Neil Brown smart acoustic current meter (SACM) to record wave statistics in addition to the conventional mean current components and temperature. It remains to be determined whether the microprocessor could handle the additional computational load involved in computing these additional wave-related quantities.

With the assistance of the manufacturer algorithms for computing the dominant wave period and the characteristics of the wave orbital ellipse in the horizontal plane were implemented in the microprocessor aboard the current meter. After five trials in the tow tank facility of the National Water Research Institute, we eliminated the obvious errors to the point where current meters outfitted with the wave statistics microprocessor were considered suitable for field evaluation. In the following, we describe a field experiment in Lake St. Clair designed to compare the wave parameters derived from the current meters with those determined from standard procedures, discuss the results of the evaluation and make recommendations for improvements in the instrumentation.

METHODS

Current meters outfitted with the facility for recording currents and wave statistics were fixed to a rigid bottom supported mount at a nominal height above the bottom of 1 m at stations 505 and 506 and at the heights of 0.35 and 4.72 m at station 501 (Figure 1). Over the two-week long field experiment the sum over an 8-minute burst of the squares of the individual 0.5-s readings of the (magnetic) east component of current, the sum of north components, sum of the products of the east and north components, and the number of zero crossings of the east and north components of flow were recorded along with the standard averages of east and north components of flow and the water temperature. The bursts were taken at either 2 or 0.5-hr intervals.

At the same time, supporting data such as the wave period and significant height were observed at station 501 by a wave and tide recorder of Sea Data manufacture. The time histories of these variables are shown in Figure 2 along with the significant wave orbital velocity inferred from linear theory for the bottom depth. Wave data obtained from the Marine Environment Data Service (MEDS) at station 24 are shown for comparison. Significant quantities are a factor of four larger than RMS quantities. As seen from Figure 2, the major autumnal wave events of the 1986 field season occurred on October 6 and 15, shortly before the evaluation period. However, storms of intermediate intensity were experienced on October 30 and November 4, 1986. The associated wind speeds and directions measured at the bottom supported tower of station 501 are shown in Figure 3a. Of more relevance to the wave direction of interest here is the fetch-weighted wind direction. According to the theory of Donelan et al. (1985), the dominant wave energy direction can be determined for any wind direction given the distribution of fetch at the observation point. In the case of locations in the southeastern corner of Lake St. Clair, dominant wave directions are parallel to wind directions except in the southwest and northeast directions where small differences are apparent.

In the preparation of plots of the wave statistics derived from the current meters such as the wave directions of Figure 3b, it was noticed that occasional spikes occurred in the data sequences. Therefore, in the presentation of Figure 3b, the irregularities were removed by hand and by inserting linearly interpolated values for the erroneous data. After smoothing, a close correspondence between the fetch-weighted directions and the wave directions are evident especially the abrupt shifts in wave direction just following the two storm events. The problem of the randomly spaced spikes was brought to the attention of the manufacturer of the SACM. After considerable investigation it was found that for an unknown reason occasional shifts in the data sequence are processed by the current meter's computer. This shifting had apparently been previously unnoticed by the manufacturer and others as it contributed little error to the mean quantities. However, the squaring of the data in the modified version greatly magnified this sequencing error. Because there is possible contamination of the current meter data, no further analysis of the data at stations 505 and 506 was undertaken.

Instead, attention was focussed on the two current meters at station 501. At this location, an auxilliary system recorded the primary 0.5-s current data. Only 58 episodes over the two-week period could be retrieved. From the individual readings the data shifts were identified and corrected by either shifting back into the correct sequence or by interpolation from adjacent scans. Thus, error-free current statistics were computed for each of the 58 bursts. The synthetic current meter statistics were checked for validity with those cases known to be free of data shifts and were found to be within ±1 mm/s in mean flow. Parenthetically, it was found that the microprocessor of the SACM sometimes computed an additional zero crossing. This is thought to be due to the sign of zero so that a tangent at zero and from either one side or the other of the axis is counted as a zero crossing. Since the number of samples in a burst is large (960), the occasional extra zero crossing does not result in serious error.

The corrected 0.5-s data for each of the 58 episodes at station 501 were subjected to cross spectral analysis, permitting the peak wave frequency (period) to be identified and the wave direction and orbital motion to be estimated. In the computation of the latter quantities wave spectral densities were integrated over the frequency band from 0.13 to 0.28 hz, an interval shown by cross spectral analysis between the two levels of current to contain coherent wave energy during the experimental period. Wave directions are computed from the band averaged spectral densities and cospectra from standard formulae.

Finally, in Appendix I, the expressions used to derive wave parameters from the recorded data are given.

FIELD RESULTS

(a) Wave Orbital Motion

A scatter plot of 116 estimates of RMS wave orbital motion from the synthetic wave statistics against the wave orbital speeds from the spectral analysis of the high speed data demonstrate close correspondence in Figure 4. As might be expected in a well exposed location in a shallow lake, most of the variance is contained in the wave band. The small portion of the flow variance outside the band explains why the current meter always slightly overestimates (3%) the true RMS orbital motion.

(b) Wave Direction

Somewhat poorer correspondence between the spectrally determined and microprocessor-based directions is evident from the scatter of points in Figure 5. Much closer agreement holds when the orbital motion exceeds the mean flow.

(c) Wave Period

The poorest agreement of the three wave parameters is found in wave period which demonstrates considerable deviation in Figure 6. The simple zero crossing method should be influenced by the mean flow. Figure 7 indicates that the RMS orbital speed must be about twice the mean speed before the relative error in period is acceptable.

Donelan (1973) has suggested a method of measuring the dominant wave frequency by summing the squares of differences of successive readings. A comparison between periods using Donelan's algorithm, shown in Figure 8, indicates that this technique does not offer substantial improvement. The main difference is that the sum of squares of differences tends to reduce the errors of the outlying points. On Figure 7, 84 points are plotted whereas on Figure 8, 114 episodes out of a possible 116 have periods less than 6 s. Any method based on successive differences depends heavily on the precision of the numbers. It is possible that the 12-bit resolution of the current meter is not sufficiently high for this method to be reliable.

CONCLUSIONS AND RECOMMENDATIONS

In the course of field testing of an enhanced microprocessor-based current meter designed to record wave parameters as well as flow a fault in current meter was discovered that results in occasional random errors in the current speed, direction and temperature readings. It is recommended that the source of the error be found and corrected before further field deployment on SACM instruments be undertaken.

In application to the coastal and nearshore zones or in shallow wave dominated lakes, wave orbital motions are likely to be overestimated by approxiately 3% and RMS wave direction deviations are given to ±19 degrees overall. While both these cases are considered to be reasonable tolerances, the situation is less satisfactory with respect to wave period where only in the cases when the RMS orbital velocity is twice the mean speed are errors acceptably low. Since the method of Donelan (1973) did not result in much improvement, it is recommended in cases where wave period is essential or the above conditions are too restrictive, that the velocity component spectra be computed by a more powerful microprocessor and either the frequency of the maximum spectral density or a limited number of spectral estimates be recorded.

Although the wave statistics in the present study are capable of resolving the ellipticity of the wave orbit in the horizontal plane, this parameter was not tested as it is seldom used in limnological studies.

Provision of a microprocessor capable of being programmed in a high level computer language would offer the user valuable flexibility. For example, in our studies it would have been extremely useful to be able to record means and standard deviations of light extinction measurements from an optical transmissometer located adjacent to the current meter.

ACKNOWLEDGEMENTS

The authors wish to acknowledge the assistance of J. Morrison of EG&G in the development of the microprocessor code, R. Taylor of the Marine Environmental Data Services for kindly supplying additional wave data and R.C. McCrimmon for displaying the MEDS data.

REFERENCES

Bull, J.A. and J. Valdmanis. Experience with Neil Brown SACM current meters in Lake St. Clair, Canada/U.S.A. 1985. In Proceedings of the IEEE Third Working Conference on Current Measurements, June 22-24, 1986, Arlie Virginia, pp. 45-51, IEEE, New York 1986.

Christoffersen, J.B. and J.G. Jonsson, 1985. Bed friction and dissipation in a combined current and wave motion. Ocean Engng., 12: 387-424.

Donelan, M.A., J. Hamilton and W.H. Hui, 1985. Directional spectra of wind-generated waves. Phil. Trans. R. Soc. Lond. A 315: 509-562.

Donelan, M.A., 1973. A method for the automatic measurement of wave frequency. J. Fisheries Res. Bd. Can., 33(10): 2318-2322.

Grant, W.D. and O.S. Madsen, 1979. Combined wave current interaction with a rough bottom. J. Geophys. Res., 84(C4): 1797-1800.

Hamblin, P.F., Y.M.R. Marmoush and F.M. Boyce, 1987. Field evaluation of an electromagnetic current meter based vertical profiler. J. Geophys. Res. 92(C11): 11867-11872.

APPENDIX I

Wave period, P, is computed from the zero crossings on the x-axis, Nx, the y-axis crossings, Ny, the number of samples, N, and the sampling interval, Δt, according to

$$P = 2N\Delta t/MAX(Nx,Ny).$$

Similarly, the period taken from Donelan's (1973) method is the lessor of the two periods along the axes.

If the mean east component flow is $\overline{X}$ and the sum of squares of the east component is X2 over the burst sample, then the variance of the east component is $Var_x = X2/N - \overline{X}^2$. Similarly, $Var_y = Y2/N - \overline{Y}^2$ and $Var_{xy} = XY/N - \overline{X}\,\overline{Y}$ where XY is the sum of the products of x and y components. If we define an intermediate quantity,

$$R = \sqrt{(Var_x + Var_y)^2 - 4(Var_x\, Var_y - Var_{xy}{}^2)}$$

then the RMS orbital speed is

$$U_{RMS} = \sqrt{(Var_x + Var_y + R)/2}.$$

The direction of wave propagation, α, is given by the expression,

$$\alpha = ATAN^{-1}((Var_y - R)/ - Var_{xy}).$$

It is noted that in the wave direction plots of Figure 3b, 180° is either subtracted or added to the above estimate depending on the minimum difference between the wave direction and wind speed.

It is often useful to know the average speed which was not computed by the microprocessor. An approximation to the average speed over a burst is given by the integral

$$\frac{1}{2\pi} \int_0^{2\pi} [(\overline{X} + U_{RMS} \cos \alpha \cos \omega - U_T \sin \alpha \sin \omega)^2$$

$$+ (\overline{Y} + U_{RMS} \sin \alpha \cos \omega + U_T \cos \alpha \sin \omega)^2]^{1/2} \, d\omega$$

where $U_T = \sqrt{(Var_x + Var_y - R)/2}$.

Numerical evaluations of the integral were on the average 10% less than the true mean speed.

LIST OF FIGURE CAPTIONS

Figure 1. Experimental site, Lake St. Clair.

Figure 2. Significant wave orbital motions at bottom (cm/s), significant wave height (cm) and wave period measured at sites 501 (solid) and 24 (dashed).

Figure 3. (a) Wind direction and wind speed at site 501. Dashed line is the fetch-weighted wind direction.

(b) Observed wave direction at stations 505 and 506, October 24 to November 8, 1986.

Figure 4. RMS wave orbital speed from simulated microprocessor statistics versus RMS wave orbital speed from velocity spectra (cm/s).

Figure 5. Same as Figure 4 except for wave direction from magnetic north. The circles indicate points for the RMS orbital speed larger than the mean speed and the pluses are all other points.

Figure 6. Same as Figure 4 but for wave period in seconds based on number of zero crossings.

Figure 7. Estimated wave period (zero crossing) minus true wave period divided by true wave period against the ratio of RMS orbital motion to mean speed.

Figure 8. Same as Figure 4 but wave period estimated from sum of successive differences squared.

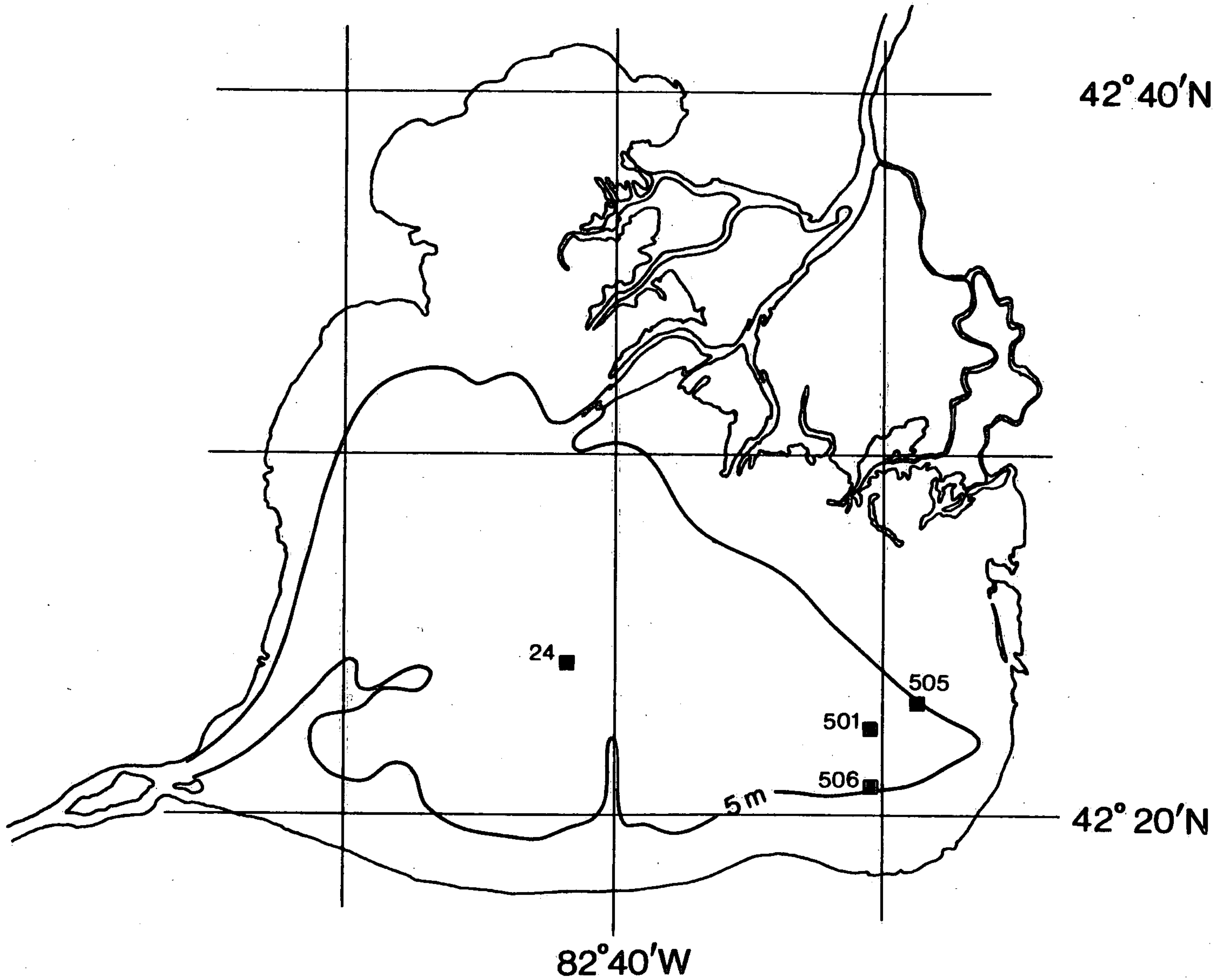
42° 40′N
42° 20′N
82° 40′W
24
505
501
506
5 m

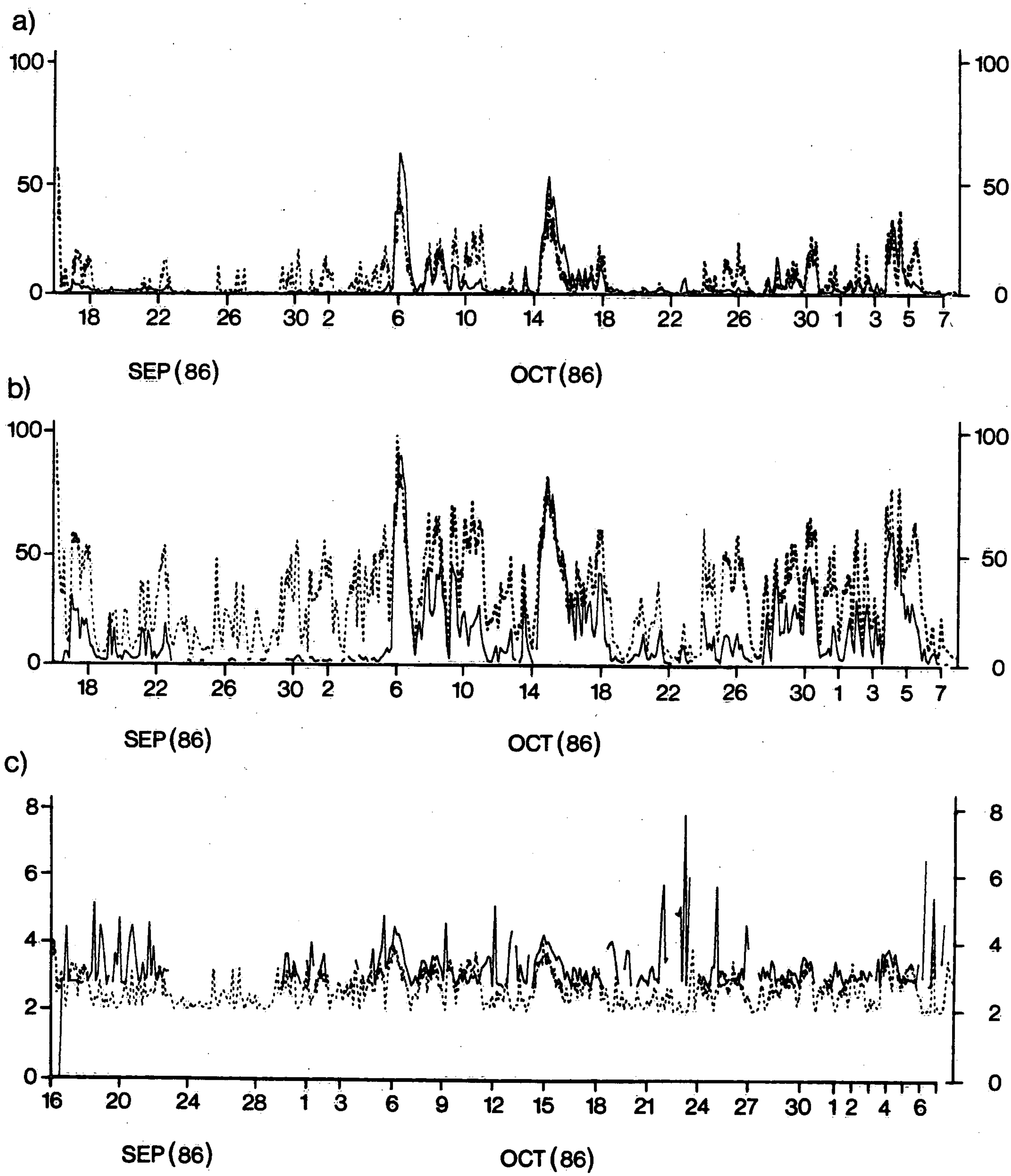
a)
100
50
0
18 22 26 30 2 6 10 14 18 22 26 30 1 3 5 7
SEP (86)
OCT (86)
b)
100
50
0
18 22 26 30 2 6 10 14 18 22 26 30 1 3 5 7
SEP (86)
OCT (86)
c)
8
6
4
2
0
16 20 24 28 1 3 6 9 12 15 18 21 24 27 30 1 2 4 6
SEP (86)
OCT (86)

2

(a)

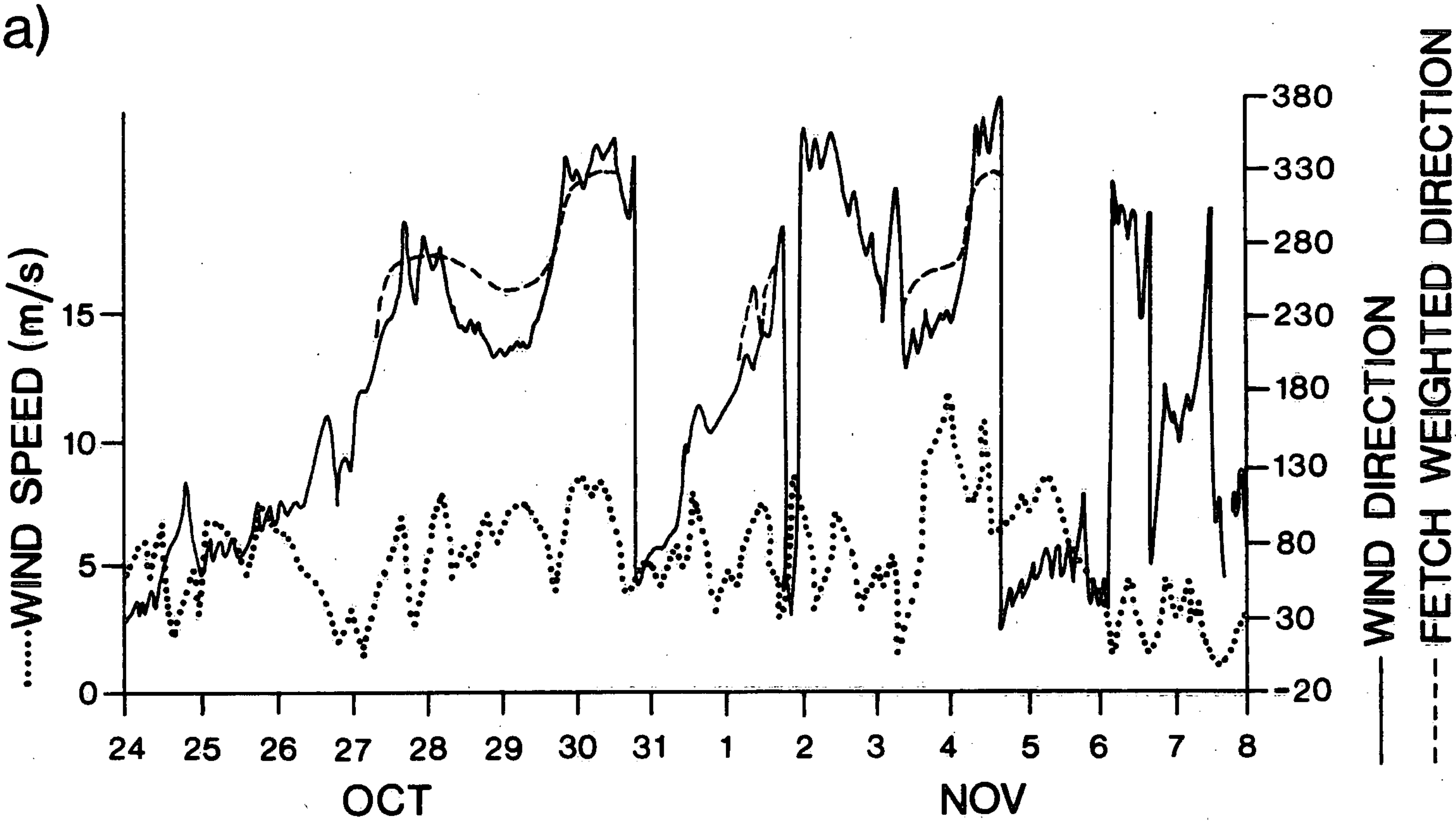
WIND SPEED (m/s)
WIND DIRECTION
FETCH WEIGHTED DIRECTION
15
10
5
0
380
330
280
230
180
130
80
30
-20
24
25
26
27
28
29
30
31
1
2
3
4
5
6
7
8
OCT
NOV

(b)

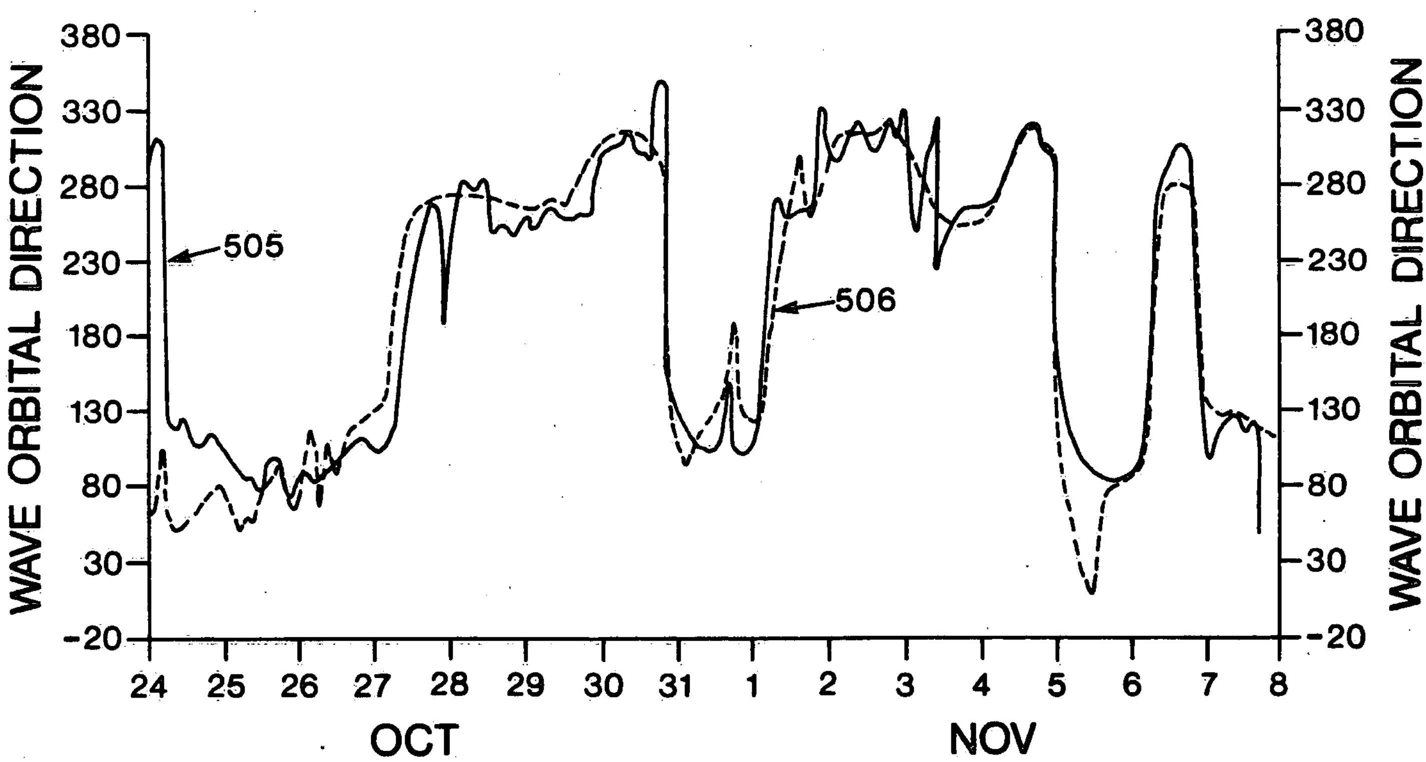
WAVE ORBITAL DIRECTION
WAVE ORBITAL DIRECTION
505
506
380
330
280
230
180
130
80
30
-20
24
25
26
27
28
29
30
31
1
2
3
4
5
6
7
8
OCT
NOV

3

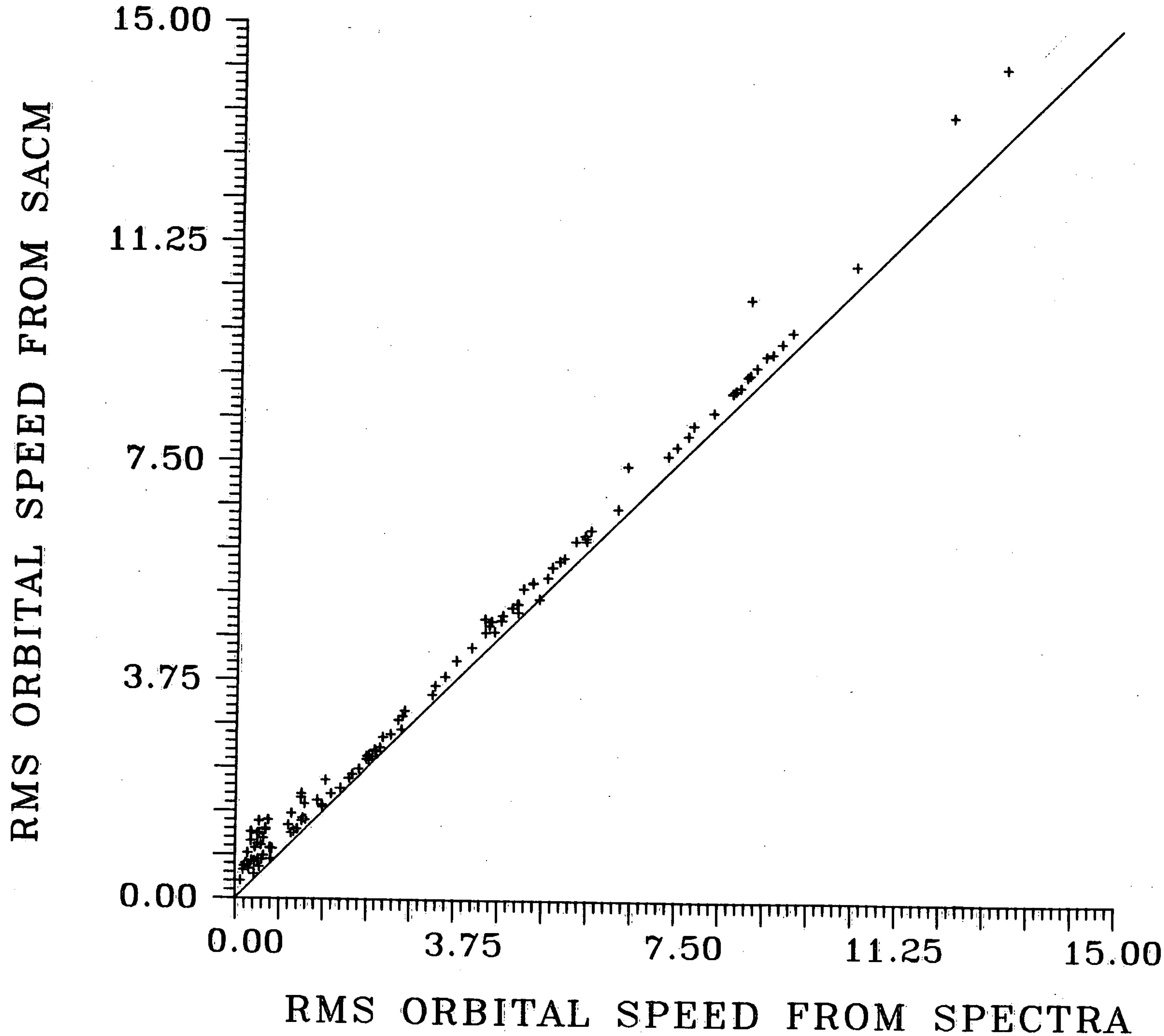
15.00
11.25
7.50
3.75
0.00
0.00
3.75
7.50
11.25
15.00
RMS ORBITAL SPEED FROM SACM
RMS ORBITAL SPEED FROM SPECTRA

4

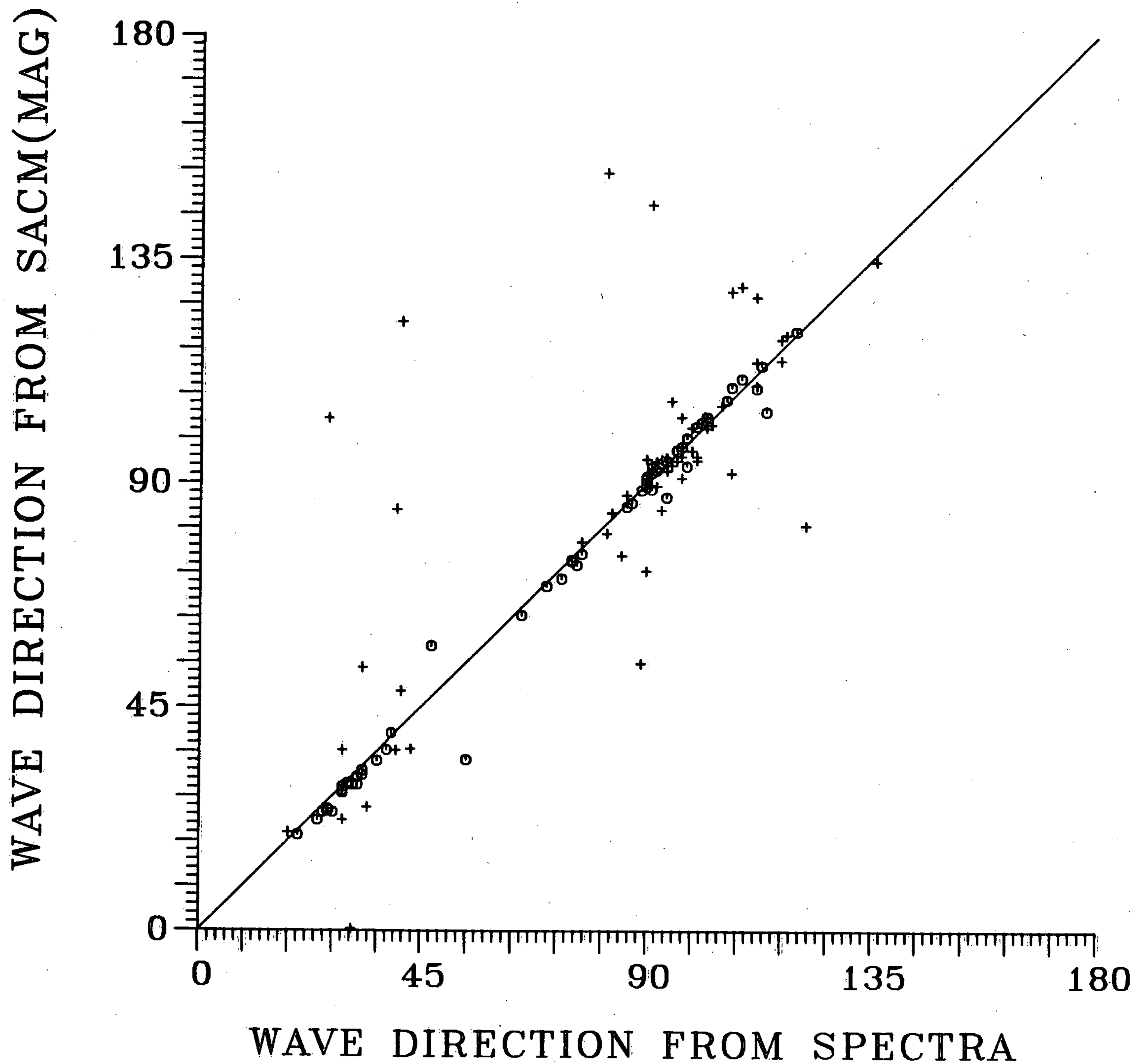

WAVE DIRECTION FROM SACM(MAG)
180
135
90
45
0
0
45
90
135
180
WAVE DIRECTION FROM SPECTRA

5

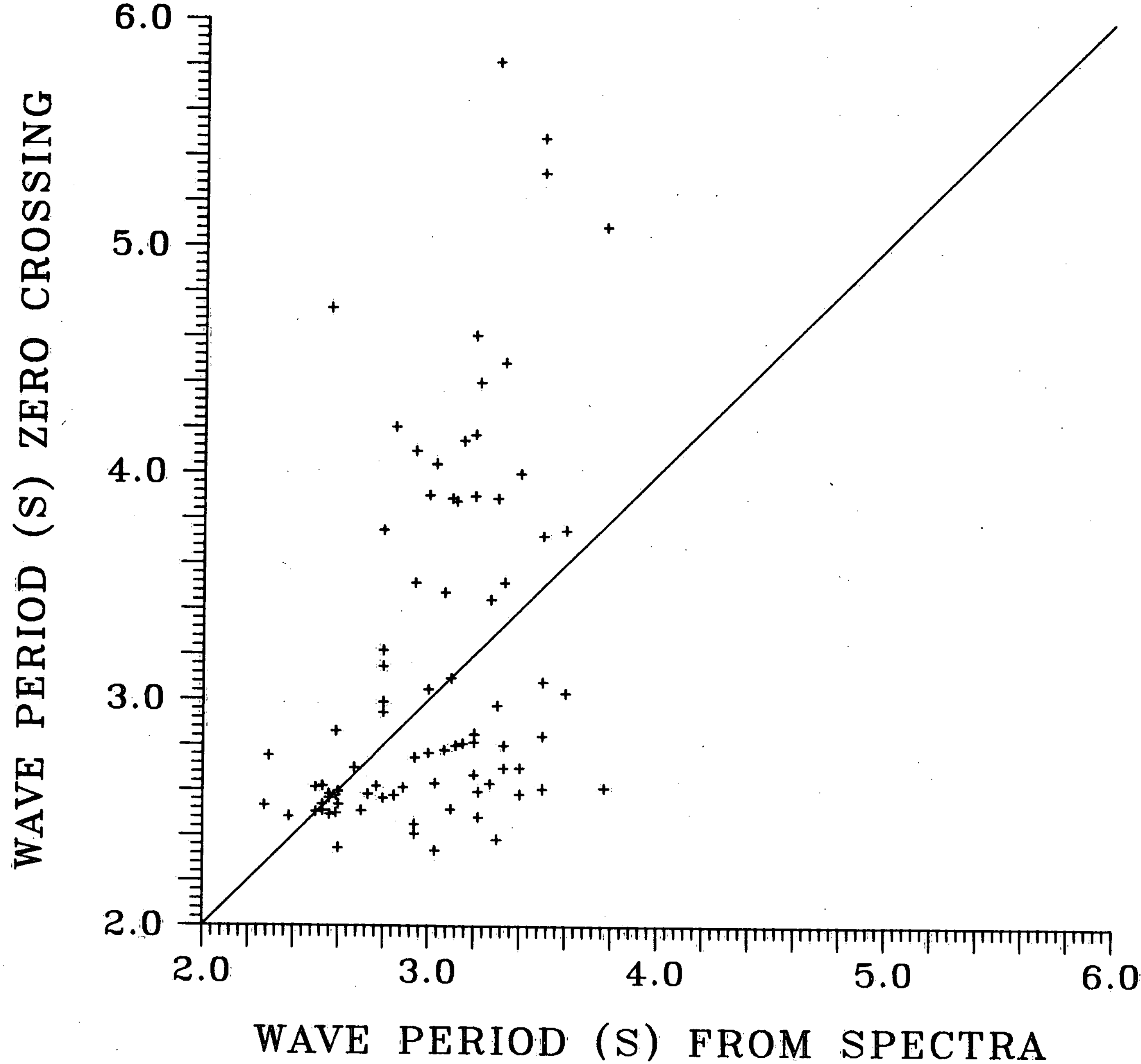
6.0
5.0
4.0
3.0
2.0
WAVE PERIOD (S) ZERO CROSSING
2.0
3.0
4.0
5.0
6.0
WAVE PERIOD (S) FROM SPECTRA

9

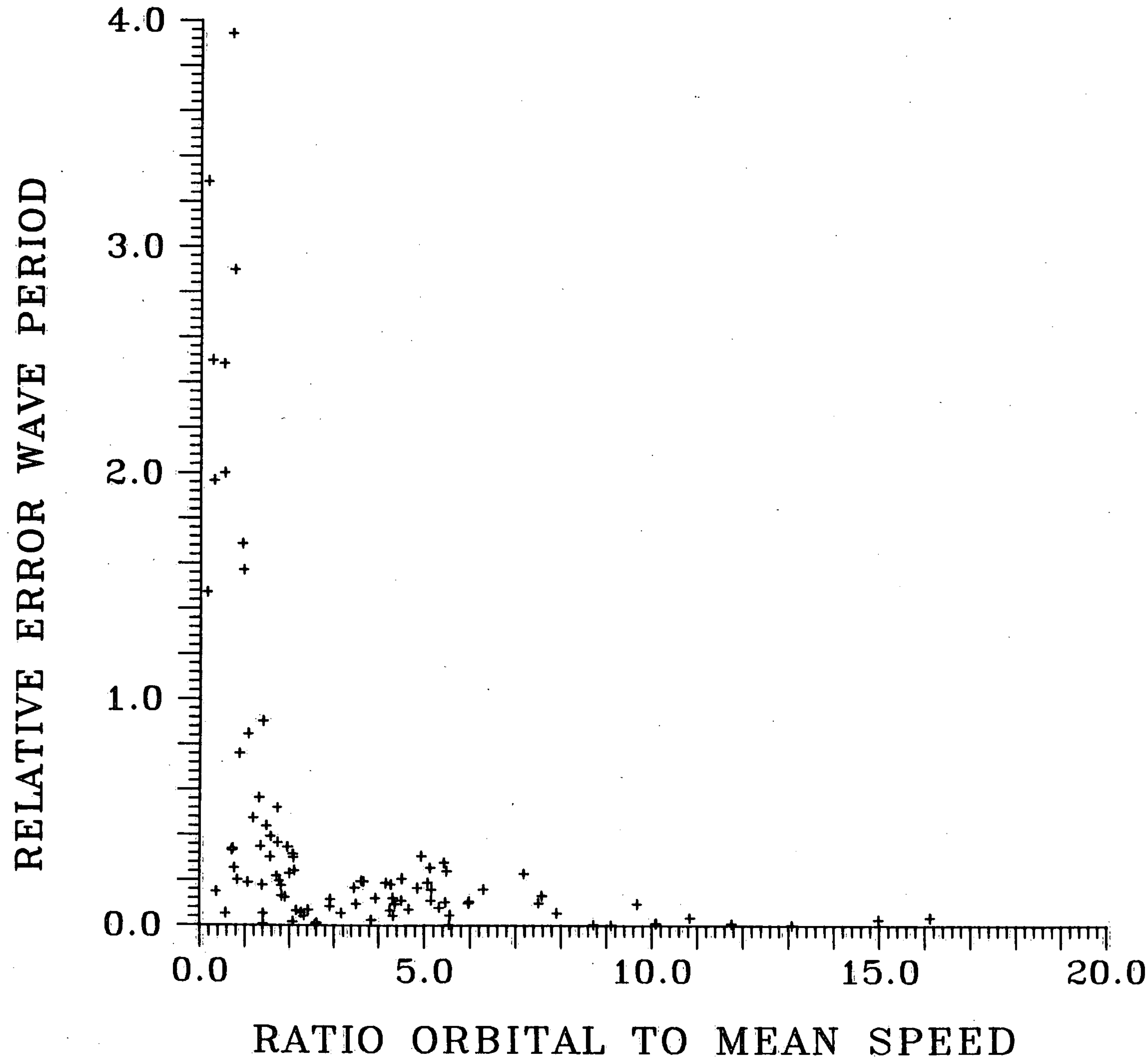

RELATIVE ERROR WAVE PERIOD
4.0
3.0
2.0
1.0
0.0
0.0
5.0
10.0
15.0
20.0
RATIO ORBITAL TO MEAN SPEED

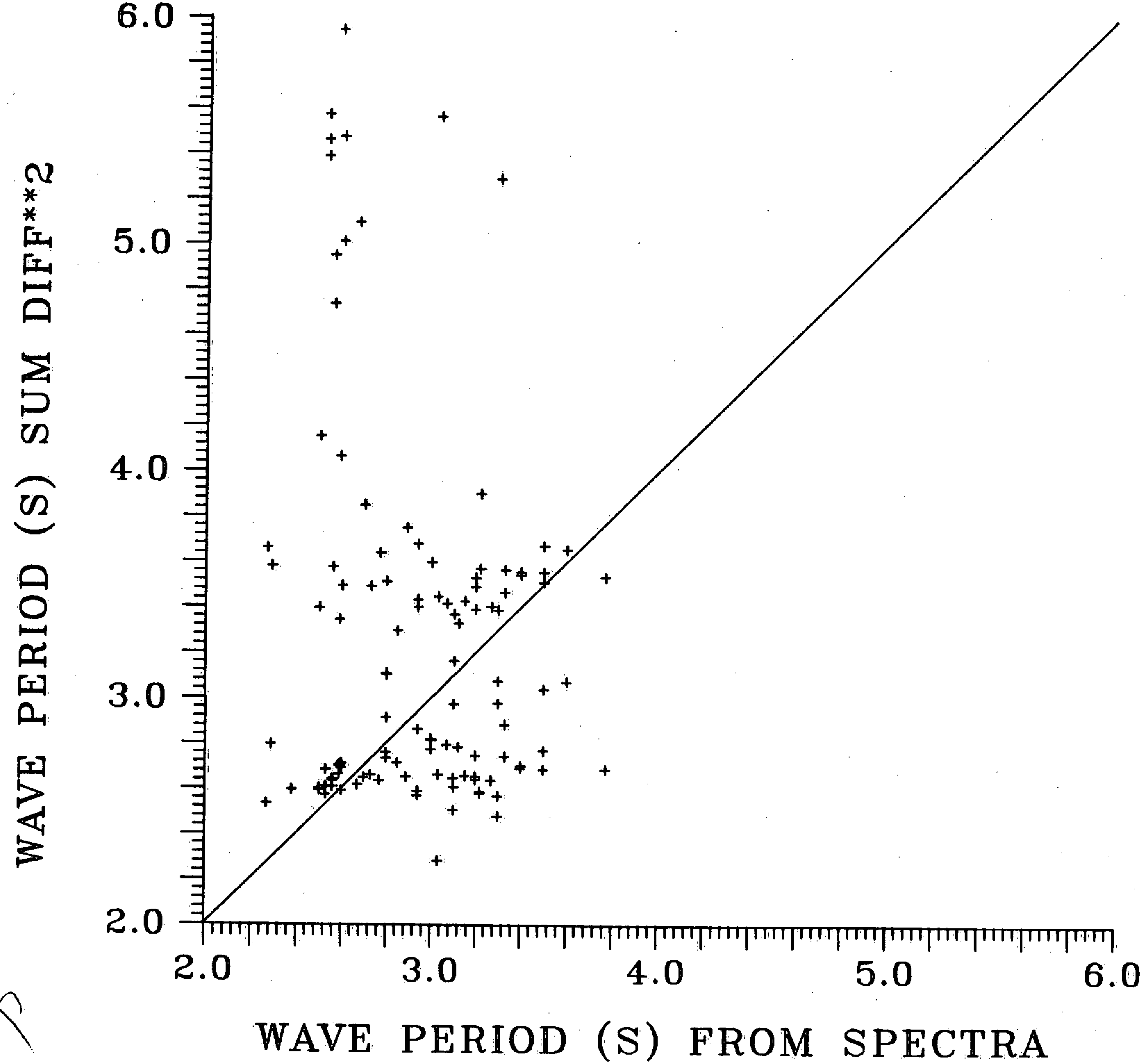
6.0
5.0
4.0
3.0
2.0
2.0
3.0
4.0
5.0
6.0
WAVE PERIOD (S) SUM DIFF**2
WAVE PERIOD (S) FROM SPECTRA